

# Extracellular MicroRNAs Activate Nociceptor Neurons to Elicit Pain via TLR7 and TRPA1

Chul-Kyu Park,<sup>1,2</sup> Zhen-Zhong Xu,<sup>1,2</sup> Temugin Berta,<sup>1,2</sup> Qingjian Han,<sup>1</sup> Gang Chen,<sup>1</sup> Xing-Jun Liu,<sup>1</sup> and Ru-Rong Ji<sup>1,\*</sup>

<sup>1</sup>Pain Signaling and Plasticity Laboratory, Departments of Anesthesiology and Neurobiology, Duke University Medical Center, Durham, NC 27710, USA

<sup>2</sup>Co-first authors

\*Correspondence: ru-rong.ji@duke.edu

<http://dx.doi.org/10.1016/j.neuron.2014.02.011>

## SUMMARY

Intracellular microRNAs (miRNAs) are key regulators of gene expression. The role of extracellular miRNAs in neuronal activation and sensory behaviors are unknown. Here we report an unconventional role of extracellular miRNAs for rapid excitation of nociceptor neurons via toll-like receptor-7 (TLR7) and its coupling to TRPA1 ion channel. miRNA-let-7b induces rapid inward currents and action potentials in dorsal root ganglion (DRG) neurons. These responses require the GUUGUGU motif, only occur in neurons coexpressing TLR7 and TRPA1, and are abolished in mice lacking *Tlr7* or *Trpa1*. Furthermore, let-7b induces TLR7/TRPA1-dependent single-channel activities in DRG neurons and HEK293 cells overexpressing TLR7/TRPA1. Intraplantar injection of let-7b elicits rapid spontaneous pain via TLR7 and TRPA1. Finally, let-7b can be released from DRG neurons by neuronal activation, and let-7b inhibitor reduces formalin-induced TRPA1 currents and spontaneous pain. Thus, secreted extracellular miRNAs may serve as novel pain mediators via activating TLR7/TRPA1 in nociceptor neurons.

## INTRODUCTION

MicroRNAs (miRNAs) are 18–25 nucleotide noncoding RNAs and bind the 3' UTRs of mRNAs to regulate gene expression posttranscriptionally (Bartel, 2004). miRNAs have been implicated in various biological roles including neurodegeneration (Eacker et al., 2009). Extracellular miRNAs are also present in circulating blood and cerebrospinal fluid in disease conditions (Lehmann et al., 2012) and binds toll-like receptor-7 (TLR7) (Fabri et al., 2012). TLR7 is activated by single-strand RNAs to initiate innate immune responses via transcriptional regulation (Takeuchi and Akira, 2010). The miRNA lethal-7 (let-7), first discovered in the nematode as a key developmental regulator (Reinhart et al., 2000), is abundant and highly conserved across species (Pasquinelli et al., 2000). Interestingly, let-7 has been detected in the cerebrospinal fluid of patients with Alzheimer's disease (Lehmann et al., 2012). Extracellular application of let-7b induces apoptosis of cortical neurons via activation of neuronal

TLR7 and myeloid differentiation factor 88 (MyD88)-dependent transcriptional regulation of TNF- $\alpha$  (Lehmann et al., 2012). miRNAs were also found in nociceptive primary sensory neurons (nociceptors) of dorsal root ganglion (DRG) to regulate pain and the expression of sodium channels (Zhao et al., 2010). However, the unique role of secreted extracellular miRNAs in modulating the activation and excitability of sensory neurons and sensory behaviors is virtually unknown.

Recently, we have shown that TLR7 is expressed by small-diameter DRG neurons (Liu et al., 2010) that are responsible for the sensations of pain and itch (Basbaum et al., 2009; Liu and Ji, 2013; Woolf and Ma, 2007). Furthermore, the synthetic TLR7 ligands imiquimod and loxoribine induced rapid inward currents and action potentials in DRG nociceptor neurons (Liu et al., 2010). However, the endogenous ligands of TLR7 remain to be identified. In this study, we evaluated whether extracellular miRNAs could serve as TLR7 agonists to rapidly activate DRG neurons and elicit pain and further determined functional coupling between TLR7 and ion channels.

## RESULTS

### Specific miRNAs Induce Inward Currents in DRG Neurons via TLR7 and TRPA1

We first tested whether let-7b, which contains immune stimulatory GUUGUGU motif (Figure 1A) for the activation of TLR7 (Heil et al., 2004), would elicit electrophysiological responses in DRG neurons using patch-clamp recordings. Exposure of dissociated DRG neurons to let-7b, at the concentration of 7  $\mu$ M (50  $\mu$ g/ml), induced robust inward currents in small-diameter DRG neurons (<25  $\mu$ m) of wild-type (WT) mice, and these currents were abolished in *Tlr7*<sup>-/-</sup> mice, indicating a TLR7-dependent action (Figures 1B and 1C). However, the mutant oligoribonucleotide (Mut. oligo) with reduced GU content (Figure 1A) (Lehmann et al., 2012) had no effects (Figures 1B).

We next asked whether TRPA1, expressed by TRPV1-positive nociceptors (Liu et al., 2010; Story et al., 2003), is involved in miRNA-induced inward currents. We found all the let-7b-responsive neurons also responded to the TRPA1 agonist AITC (Jordt et al., 2004) (Figure 1B). Notably, let-7b-induced inward currents were completely blocked by the TRPA1 antagonist HC030031 (100  $\mu$ M) and eliminated in *Trpa1*<sup>-/-</sup> mice (Figures 1B and 1C). TLR7 agonist loxoribine (200  $\mu$ M) also evoked inward currents (Figure 1B), which were abolished in *Tlr7*<sup>-/-</sup> and *Trpa1*<sup>-/-</sup> mice (data not shown).

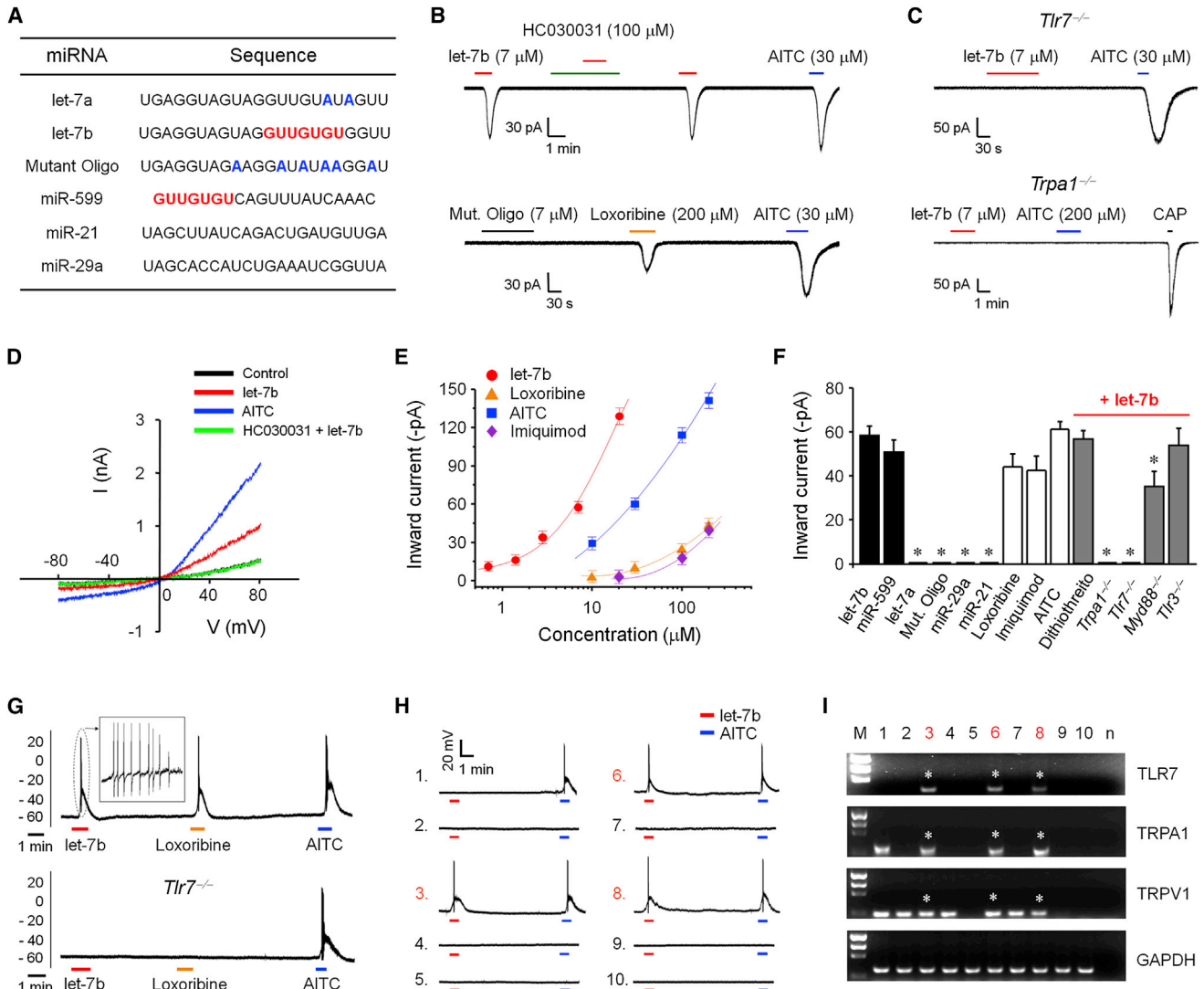


**Figure 1. let-7b Induces Inward Currents and Action Potentials in Small-Sized DRG Neurons via TLR7 and TRPA1**

(A) Sequences of miRNAs tested in this study. The GUUGUGU motif is underlined. In mutant oligonucleotides (Mut. Oligo) and let-7a, the mismatched nucleotides (compared with let-7b) are highlighted in blue. (B and C) Inward currents induced by let-7b, loxoribine, and AITC. Note that let-7b-induced inward currents are blocked by HC030031 (B) and abolished in *Trp1*<sup>-/-</sup> and *Trpa1*<sup>-/-</sup> (C) mice. Mut. Oligo fails to evoke any currents. We recorded 15–25 neurons in each condition. (D) I/V curves elicited by let-7b (7  $\mu$ M) and AITC (200  $\mu$ M). n = 5 patches for each condition. let-7b and AITC elicit similar I/V curves with the reversal potential of 0 mV. let-7b-induced current is suppressed by HC030031 (100  $\mu$ M). n = 5 neurons. (E) Dose-response curves showing the amplitudes of inward currents induced by let-7b, loxoribine, imiquimod, and AITC. n = 5–18 neurons. Note a left shift of the let-7b curve. (F) Summary of amplitudes of the inward currents under all the experimental conditions (n = 5–25 neurons). The concentrations are 7  $\mu$ M for let-7a, let-7b, and Mutant Oligo, 8  $\mu$ M for miR-599, 10  $\mu$ M for miR-29a and miR21, 30  $\mu$ M for AITC, 200  $\mu$ M for loxoribine and imiquimod, and 5 mM for dithiothreitol. \*p < 0.05, compared to let-7b, n = 5–25 neurons. The results are represented as mean  $\pm$  SEM. (G) Action potentials induced by let-7b, loxoribine, and AITC in DRG neurons. n = 5–15 neurons. Note that let-7b-induced action potentials are eliminated in all 15 neurons from *Trp1*<sup>-/-</sup> mice. (H and I) Current-clamp recording (H) and single-cell RT-PCR (I) in ten small-sized DRG neurons. Note that let-7b induces action potentials only in TLR7-expressing neurons. Three neurons (3, 6, and 8, highlighted in red) respond to let-7b (7  $\mu$ M) with action potentials and also express *Trp1*, *Trpa1*, and *Trpv1* mRNAs (indicated with \*). M, molecular weights; n, negative control. Asterisks indicate TLR7-positive neurons.

I/V curve analysis further revealed that let-7b-evoked currents possess typical property of TRP channels: they are suppressed by HC030031 and have the reverse potential of 0 mV (Figure 1D). Dose-response curves of inward currents showed a left shift of the let-7b-elicited curve, compared to that elicited by AITC, loxoribine, and imiquimod, suggesting that let-7b has the highest efficacy for TRPA1 activation. The lowest concen-

tration of let-7b that we tested to elicit inward current is 0.7  $\mu$ M (Figure 1E). The amplitudes of inward currents induced by different miRNA and synthetic TLR7 ligands are summarized in Figure 1F.

We further assessed whether miRNA-induced neuronal activation is sequence dependent. miR-599, which also contains the GUUGUGU motif (Figure 1A), elicited TLR7-dependent

current (Figure S1A available online). By contrast, miR-29a and miR-21 (lacking the GUUGUGU motif; Figure 1A) had no effects (Figure 1F; Figure S1B). Of interest, let-7a (Figure 1A), a close family member of let-7b with a single nucleotide change in the GUUGUGU motif (GUUGUAU), failed to induce any inward current (Figure 1F; Figure S1C). Together, these results suggest that GU-rich core (GUUGUGU) is critically required for inducing miRNA-induced inward currents. A database search (<http://www.mirbase.org/>) indicated that there are only a few miRNAs of *Homo sapiens* and *Mus musculus* that contain the motif (Table S1).

### let-7b Induces Action Potentials in DRG Neurons that Coexpress TLR7 and TRPA1

let-7b (7  $\mu$ M) evoked marked action potentials in DRG neurons, which were completely blocked by HC030031 and eliminated in *Tlr7*<sup>-/-</sup>-deficient neurons (Figure 1G; Figure S2A). Loxoribine but not Mut. Oligo also induced action potentials in AITC-responsive neurons (Figure 1G; Figures S2A and S2B). These data suggest that miRNA let-7b also causes excitation of sensory neurons via activation of TLR7 and TRPA1.

To further define whether TLR7 and TRPA1 are coexpressed in DRG neurons, we performed combined patch-clamp recording and single-cell PCR analysis (Liu et al., 2012a) in small-diameter DRG neurons. Around 30% of these neurons expressed TLR7, and all the TLR7-expressing neurons responded to let-7b and AITC with action potentials (Figures 1H and 1I) and inward currents (Figures S3A–S3C). These results suggest a perfect match between the expression and function of TLR7 in DRG neurons. Double staining also confirmed colocalization of TLR7 and TRPA1 in DRG neurons (Figure S3D). Of note, all the TLR7<sup>+</sup> neurons contain TRPA1, which is expressed by the TRPV1<sup>+</sup> DRG neurons (Figures 1H and 1I; Figure S3E), as previously reported (Story et al., 2003).

### Intracellular Signaling Is Not Required for miRNA-Induced Activation of DRG Neurons

MyD88 is an adaptor protein and critical for the conventional signaling of most TLRs including TLR7 and the transcription of inflammatory genes (Akira et al., 2006; Liu et al., 2012b). In *Myd88*-deficient DRG neurons, let-7b- and AITC-induced inward currents were largely intact, although the amplitudes of currents were slightly reduced compared to that of WT neurons (Figure 1F; Figure S1D). Thus, MyD88 is not essentially required for the let-7b-induced currents. Moreover, exposure of DRG neurons to inhibitors of PKA, PKC, PLC, ERK, and G proteins did not impair loxoribine-induced inward currents (Figure S1E), arguing against an involvement of intracellular signaling in the TLR7/TRPA1 interaction. Noxious compounds were shown to activate TRPA1 through covalent modification of cysteines (Macpherson et al., 2007). However, the reducing agent dithiothreitol (DTT) did not affect the let-7b-induced inward current (Figure S1F), suggesting a possible noncovalent interaction between TLR7 and TRPA1. Although TLR3 detects double-strand RNAs (Akira et al., 2006) and double-strand total RNAs from brain tissues induced inward currents in DRG neurons via TLR3 (Liu et al., 2012a), let-7b-induced inward currents are *Tlr3* independent (Figure 1F).

### let-7b Induces TRPA1-Mediated Inward Currents in HEK293 Cells

Can miRNA also activate TLR7 and TRPA1 in a heterologous cell system? To address this issue, we tested the actions of miRNA in HEK293 cells overexpressing TLR7/TRPA1. let-7b evoked robust inward currents in these cells, which were completely blocked by HC030031 (Figure 2A). Notably, let-7b had no effect in HEK293 cells overexpressing TRPA1 alone (Figure 2B), confirming that TLR7 is essential for mediating the let-7b-induced currents in HEK293 cells. In contrast, TLR7 ligand failed to induce inward currents in HEK293 cells overexpressing TLR7/TRPV1, TLR7/TRPV2, or TLR7/TRPV4 (Figure 2C). Thus, TLR7 selectively interacts with TRPA1 (but not with TRPV1, TRPV2, and TRPV4) to generate TRPA1-mediated inward currents in a heterologous cell system.

### let-7b Binds TLR7 and Enhances TLR7/TRPA1 Interaction in HEK293 Cells

Next, we investigated whether fluorescence-labeled let-7b (Cy3-let-7b) can bind TLR7 in HEK293 cells. Immunocytochemistry showed surface and cytoplasm expression of TLR7 in *Tlr7*-transfected cells but not in *Tlr7* null cells (Figure 2D). Notably, we only observed Cy3-let-7b binding on TLR7-expressing cells (Figure 2D). Triple staining of let-7b/TLR7/TRPA1 revealed colocalization of all three on the cell surface as well as in cytoplasm (Figure 2D), providing subcellular bases for TLR7/TRPA1 interaction. Coimmunoprecipitation with an anti-myc antibody in TLR7/TRPA1-myc-expressing HEK293 cells revealed both TRPA1-myc and TLR7 bands (Figures 2E and 2F), suggesting a biochemical interaction of TLR7 and TRPA1. Of interest, a brief stimulation with let-7b (7  $\mu$ M, 5 min) significantly increased the interaction of TLR7/TRPA1, as indicated by increased intensity of TLR7 band (Figures 2E and 2F).

### let-7b Induces Single-Channel Activities of TRPA1 in DRG Neurons and HEK293 Cells

To further validate functional interaction of TLR7 and TRPA1 on the cell surface, we carried out single-channel recordings in both DRG neurons and HEK293 cells. Inside-out patch recordings in DRG neurons showed that intrapipette delivery of let-7b to the extracellular surface elicited voltage-dependent single-channel opening events, and the TRP channel property was validated by the I/V curve with the reversal potential = 0 mV (Figures 3A and 3B). Inside-out patch recordings in HEK293 cells overexpressing TLR7/TRPA1 also demonstrated that let-7b could elicit HC030031-sensitive single-channel activities (Figure 3C). Similarly, loxoribine induced single-channel activities of TRPA1 (data not shown). In contrast, HEK293 cells overexpressing TLR7/TRPV1 only demonstrated single-channel activities in response to capsaicin but not let-7b (Figure 3D). Together, these results suggest that let-7b could bind TLR7 on the extracellular surface to induce single-channel activities of TRPA1.

### TLR7 Is Partially Required for the Function and Surface Expression of TRPA1 in DRG Neurons

To further assess the interaction of TLR7 and TRPA1 in DRG neurons, we evaluated TRPA1 currents in WT and *Tlr7*<sup>-/-</sup> mice. Inside-out patch recordings in DRG neurons showed a significant

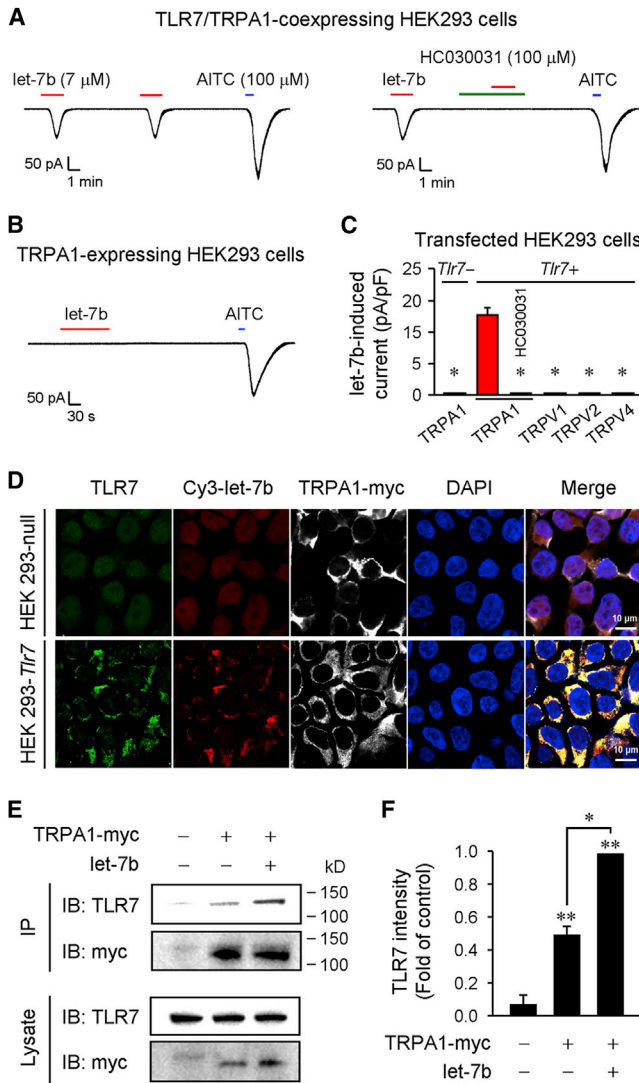


**Figure 2. let-7b Binds TLR7, Enhances TLR7/TRPA1 Interaction, and Induces TRPA1-Mediated Inward Currents in HEK293 Cells**

(A) Inward currents induced by let-7b (7  $\mu$ M) and AITC (100  $\mu$ M) in HEK293 cells overexpressing TLR7 and TRPA1. n = 15 cells. let-7b-induced current is blocked by HC030031 (100  $\mu$ M) in HEK293 cells. n = 15 cells. (B) let-7b (7  $\mu$ M) does not induce inward currents in HEK293 cells overexpressing TRPA1 alone. n = 15 cells. (C) Quantification of let-7b (7  $\mu$ M)-induced inward currents in HEK293 cells transfected with *Tlr7* and/or *Trpa1*, *Trpv1*, *Trpv2*, and *Trpv4* cDNA. n = 15 cells. (D) Triple staining of Cy3-let-7b (Cy3), TLR7 (anti-TLR7), and TRPA1-myc (anti-myc) in *Tlr7*-transfected HEK293 cells and non-transfected *Tlr7* null cells. The cell nuclei were labeled with DAPI. Scale bars, 10  $\mu$ m. Note that cy3-let-7b only binds to TLR7-expressing cells. (E and F) Coimmunoprecipitation with anti-myc antibody shows TLR7 and TRPA1-myc bands from HEK293 cells coexpressing TLR7/TRPA1. Note that let-7b (7  $\mu$ M, 5 min) increases the interaction of TLR7/TRPA1. (F) Quantification of TLR7 bands. \*p < 0.05, n = 3 separate cultures.

reduction of TRPA1 single-channel conductance and open probability in *Tlr7*-deficient neurons (Figures S4A and S4B). Immunocytochemistry also revealed a significant reduction of surface expression of TRPA1 in *Tlr7*-deficient DRG neurons (Figures S4C and S4D). As previously reported (Schmidt et al., 2009),

AITC increased the surface expression of TRPA1 in WT mice. Both the basal and AITC-induced surface expression of TRPA1 were reduced in *Tlr7*<sup>-/-</sup> mice (Figures S4C and S4D). These data indicate that TLR7 can modulate both the activity and surface expression of TRPA1.

### Endogenous let-7b Release Contributes to Formalin-Induced TRPA1 Currents in DRG Neurons

Does endogenous miRNA also play a role in modulating neuronal activity? As previously reported (McNamara et al., 2007), low concentration of formalin (0.01%) elicited TRPA1-mediated inward currents in DRG neurons (Figures 4A, S1G, and S1H). Intriguingly, the formalin-induced inward current was significantly inhibited by a let-7b inhibitor (1  $\mu$ M, anti-mmu-let-7b-5p) (Figure 4A). As expected, let-7b inhibitor blocked the let-7b- but not miR-599-induced currents (Figure 4B), validating a selective inhibition of let-7b.

### let-7b Is Highly Expressed in DRGs and Released from DRG Neurons by Neuronal Activity

To determine the expression of let-7b in different tissues, we employed quantitative RT-PCR developed by QIAGEN (see Supplemental Experimental Procedures). Of interest, let-7b levels in DRG tissue are much higher than that of spinal cord, cortex, and skin tissues (Figure 4C). To further quantify miRNA release in DRG cultures, we introduced an exogenous miRNA, *Caenorhabditis elegans* miRNA-39 (cel-miRNA-39), as a spike-in control. The basal release of let-7b in DRG cultures is around 10–25 pg/ml ( $\approx$  1.0 to 2.5 pM or  $6 \times 10^5$ – $1.5 \times 10^6$  copies/ $\mu$ l, MW = 7,133), depending on the density of the cultures (Figure 4D). This basal release is comparable to that of CGRP, a well-known pain mediator (Qin et al., 2008). Apparently, let-7b release in DRG cultures is much higher than that in CSF (5,000 copy/ $\mu$ l) (Lehmann et al., 2012). Formalin (0.01%) induced a density-dependent increase in let-7b release (Figure 4D). Activation of C-nociceptors with capsaicin and neuronal depolarization with KCl also increased let-7b release, suggesting an activity-dependent release (Figure 4E). However, AITC and the pruritogen chloroquine had no significant effects, because these agents only activate a very small population of DRG neurons (Figure 4E). Moreover, let-7b release was induced by ionomycin, an inducer of intracellular Ca<sup>2+</sup> increase (Figure 4E). The basal release of let-7a was also evident ( $\approx$  40 pg/ml) in DRG cultures. However, let-7a release was not increased by formalin, KCl, and capsaicin (Figure 4E). It is suggested that different mechanisms are involved in the release of let-7a and let-7b. We also found a quick basal release of let-7b in hindpaw skin preparation: within 5 min the let-7b concentration reached to  $3.0 \pm 0.5$  pM (n = 6 mice).

### Intraplantar Injection of let-7b Elicits Pain in Mice via TLR7 and TRPA1

Activation of small DRG neurons (nociceptors) is known to elicit pain (Basbaum et al., 2009; Caterina and Julius, 2001; Hucho and Levine, 2007; Woolf and Ma, 2007). TRPA1 is an ancient molecule for chemosensation (Kang et al., 2010) and activation of TRPA1 triggers pain in rodents (Bautista et al., 2006; Patapoutian et al., 2009; Story et al., 2003). We investigated whether extracellular (intraplantar) delivery of miRNAs would induce

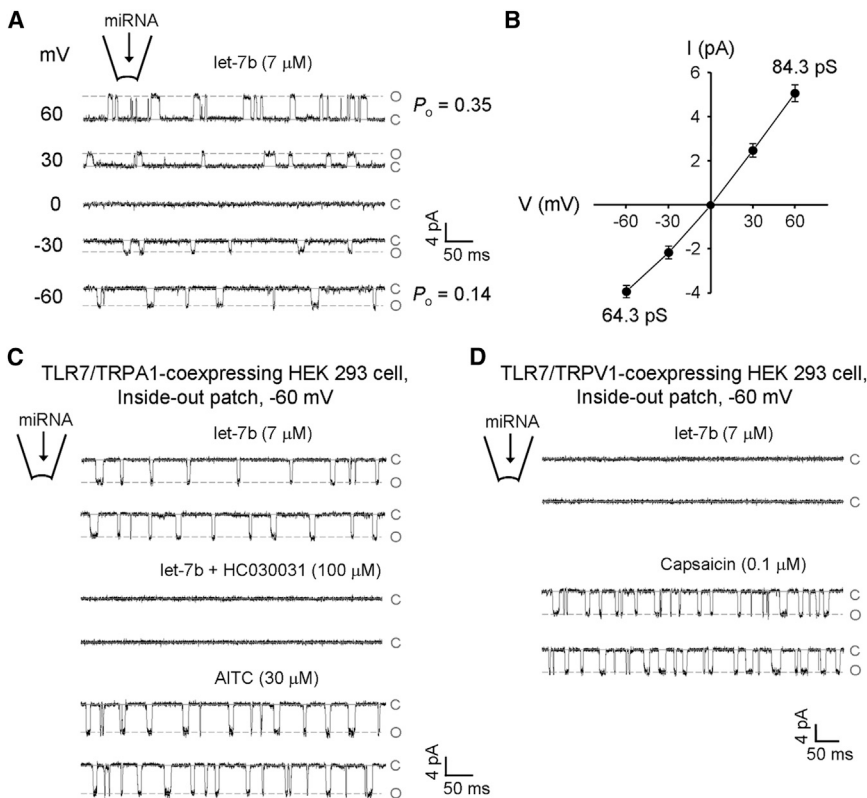


**Figure 3. let-7b Induces Single-Channel Activities of TRPA1 in DRG Neurons and Heterologous HEK293 Cells**

(A) Inside-out patch recordings in membrane excised from small-sized DRG neurons. let-7b, delivered through recording pipette, induces single-channel currents. The probability of channel opening ( $P_o$ ) at +60 and -60 mV is  $0.35 \pm 0.07$  and  $0.14 \pm 0.05$ , respectively. EGTA (1 mM) was included in the pipette solution to prevent desensitization and inactivation. c, closed state; o, open state. (B) I/V curve of let-7b-induced single-channel activities in DRG neurons. The average single-channel currents obtained in 1 min were plotted against voltages. (C) Inside-out patch recordings (-60 mV) in membrane excised from TLR7/TRPA1 overexpressing HEK293 cells. let-7b (7  $\mu$ M, through recording pipette) induces single-channel currents, which are blocked by HC030031. After washout, bath application of AITC (30  $\mu$ M) also elicits single-channel activities. (D) Single-channel activities elicited by capsaicin (100 nM) but not by let-7b (7  $\mu$ M) in inside-out patches from HEK293 cells overexpressing TLR7/TRPV1.  $n = 5$  patches for each condition.

pain-like behaviors in mice. Compared to Mut. Oligo, let-7b elicited rapid and transient (<5 min) spontaneous nociceptive pain in mice (Figure 4F), as revealed by licking and lifting behaviors of mice. These behaviors are dose dependent, peaking at the dose of 30  $\mu$ g (Figure 4F). Notably, let-7b-evoked nociceptive pain was abolished in *Tlr7*<sup>-/-</sup> mice, reduced in *Trpa1*<sup>-/-</sup> and *Myd88*<sup>-/-</sup> mice, but unaltered in *Trpv1*<sup>-/-</sup> mice (Figures 4F and 4G). Consistently, intraplantar pretreatment of HC030031 dose dependently suppressed let-7b-evoked spontaneous pain in wild-type mice (Figure 4I). Furthermore, at a low dose (1  $\mu$ g, i.e., 9.3  $\mu$ M in 15  $\mu$ l), let-7b induced persistent (>3 hr) and TRPA1-dependent mechanical allodynia (Figure 4J). Strikingly, at the dose of 30  $\mu$ g, let-7b induced long-lasting (>5 days) mechanical allodynia, which was reduced in *Tlr7*<sup>-/-</sup> and *Trpa1*<sup>-/-</sup> mice (Figures 4K and 4L), as well as in *Myd88*<sup>-/-</sup> but not in *Trpv1*<sup>-/-</sup> mice (data not shown). Intraplantar pretreatment of let-7b inhibitor reduced low-dose formalin (0.5%)-induced spontaneous pain in both phases (Figure 4M), suggesting an essential role of endogenous let-7b in inflammatory pain. Low-dose formalin (0.5%)-induced inflammatory pain was also reduced in *Tlr7*<sup>-/-</sup> mice (Figure 4N). Thus, extracellular let-7b is both sufficient and required for inducing inflammatory pain via the activation of TLR7 and TRPA1.

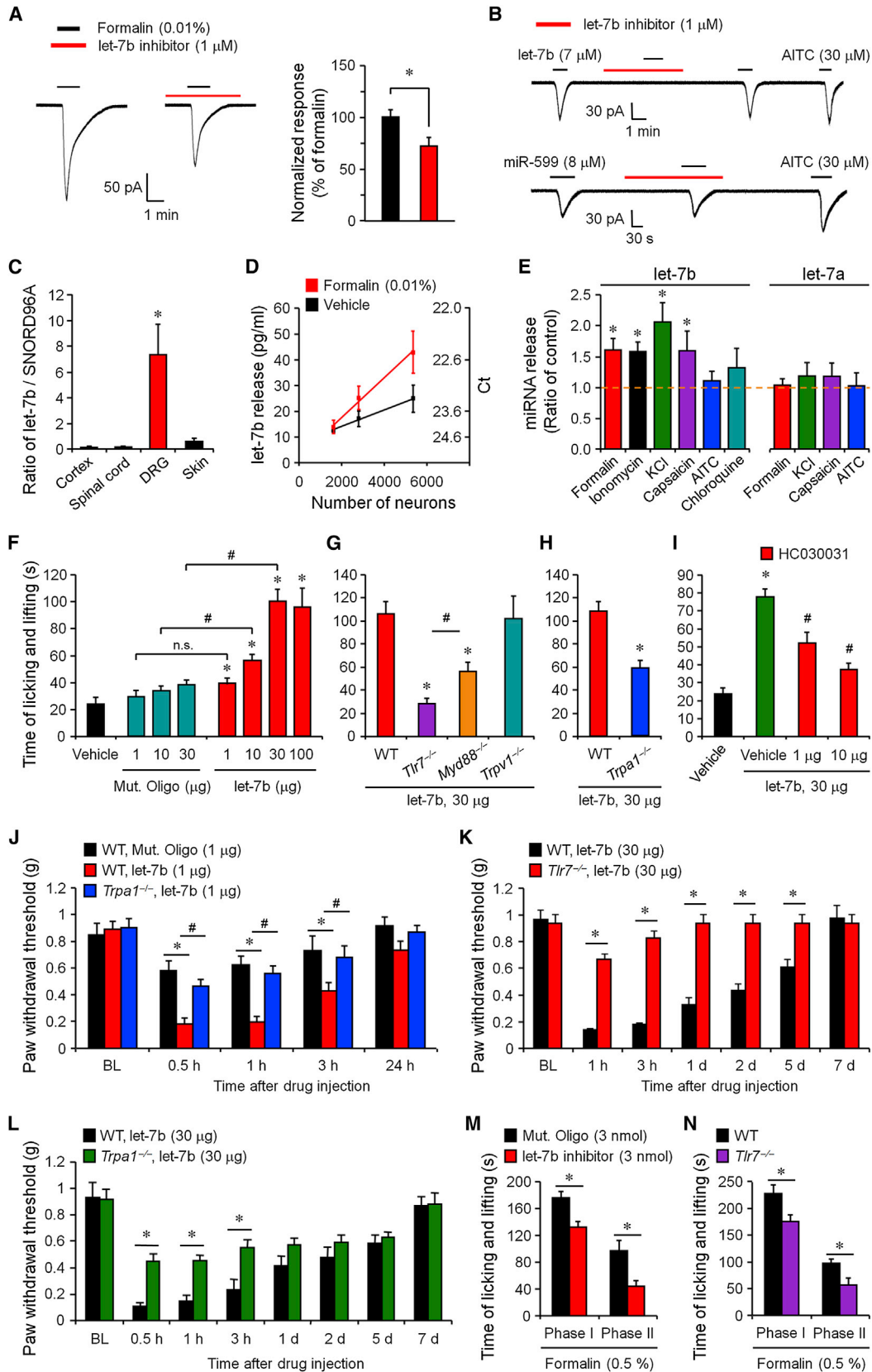
## DISCUSSION

We have identified an action of extracellular miRNAs (e.g., let-7b) for direct activation and excitation of nociceptor neurons. let-7b induced rapid (within a minute) inward currents and actions

potentials, and these effects require TLR7 but not TLR3. We also demonstrated that let-7b binds TLR7 on the surface of TLR7-expressing HEK293 cells.

Notably, let-7b is more potent than the synthetic TLR7 agonists loxoribine and imiquimod in inducing inward currents in DRG neurons and is also sufficient to induce TLR7-dependent inward currents in heterologous HEK293 cells. We found that miRNA-induced neuronal activation is sequence dependent and requires the GUUGUGU motif. Thus, miR-599 but not miR-29a and miR-21 evoked TLR7-dependent inward currents. Strikingly, let-7a, a close family member of let-7b, failed to induce any inward current, although both were shown to induce TLR7 and MyD88-dependent TNF- $\alpha$  release in immune cells (Lehmann et al., 2012). Thus, the extracellular actions of miRNAs are highly selective.

Another important finding of this study is that we identified a functional interaction of TLR7 and TRPA1 in both DRG neurons and HEK293 cells. First, TLR7 is completely colocalized with TRPA1 in small TRPV1-expressing DRG neurons. Second, let-7b-induced inward currents (with reverse potential of 0 mV) and action potentials were abolished in *Trpa1*-deficient DRG neurons and blocked by the TRPA1 antagonist HC030031. In contrast, let-7b failed to evoke inward currents in HEK293 cells overexpressing TLR7/TRPV1, TLR7/TRPV2, and TLR7/TRPV4, supporting a selective interaction of TLR7 with TRPA1. Third, TLR7 and TRPA1 can be coimmunoprecipitated in HEK293 cells, and this biochemical interaction of TLR7/TRPA1 was enhanced in response to let-7b stimulation. Fourth, inside-out recordings in DRG neurons and HEK293 cells demonstrated that let-7b was sufficient to induce single-channel activities of TRPA1 in these cells, supporting a functional interaction of TLR7/TRPA1 on the extracellular surface. Fifth, intracellular signaling (e.g.,



(legend on next page)

MyD88, PKA, PKC, PLC, and MAPK signaling) is dispensable for this interaction. Finally, TRPA1 single-channel activities and surface expression were reduced in *Tlr7*-deficient DRG neurons. Although all these lines of evidence support a functional interaction of TLR7 and TRPA1, further studies are needed to investigate protein-protein interaction between TLR7 and TRPA1.

Activation of TRPA1 in peripheral terminals of nociceptive neurons is known to evoke pain (Bautista et al., 2006; Patapoutian et al., 2009; Story et al., 2003). Intraplantar injection of let-7b also elicited rapid nocifensive pain via TLR7 and TRPA1 but not TRPV1. Moreover, let-7b induced persistent mechanical allodynia through TLR7 and TRPA1. Of interest, let-7b is highly enriched in DRG tissues and endogenous let-7b can be released from DRG neurons in an activity-dependent manner. Although our findings point to an unconventional signaling of TLR7 via TRPA1, we should not rule out the role of MyD88, especially in the maintenance phase of persistent pain. We should also point out the discrepancy between the let-7b concentrations for eliciting physiological effects ( $\mu\text{M}$ ) and the let-7b concentrations detected in DRG culture medium (pM). Such discrepancy was also found for CGRP (pM versus  $\mu\text{M}$ ) (Qin et al., 2008), a well-known pain mediator. Given the facts that (1) RNAs are generally unstable and (2) in vivo local concentrations of let-7b near axons should be much higher than that in culture medium, let-7b may reach physiological concentrations ( $\mu\text{M}$ ) after tissue injury to activate TLR7 and TRPA1. Importantly, let-7b inhibitor significantly reduced formalin-induced inflammatory pain.

In summary, we have demonstrated an unconventional extracellular role of specific miRNAs with the GUUGUGU motif (e.g., let-7b) for direct activation and excitation of nociceptive sensory neurons to evoke pain via TLR7 and TRPA1. Thus, secreted miRNAs may represent a new class of pain mediators. Secreted let-7b was implicated as a biomarker for disease (Lehmann et al., 2012). Also, let-7b changes in DRGs and circulation were found in chronic pain conditions (Orlova et al., 2011; von Schack et al., 2011; Zhao et al., 2010). Future studies are necessary to determine the tissue origins of miRNAs (e.g., let-7b) detected in circulation.

## EXPERIMENTAL PROCEDURES

See a detailed description in the [Supplemental Experimental Procedures](#).

## Reagents

We purchased miRNAs from Integrated DNA Technologies, fluorescence-conjugated siRNA (Cy3-let-7b) from Sigma, and let-7b inhibitor from QIAGEN.

## Animals

Knockout mice lacking *Tlr7*, *Tlr3*, *Trpa1*, *Trpv1*, and *Myd88* and corresponding WT control mice (B6129PF2/J background for *Trpa1*; C57BL/6 background for *Tlr7*, *Tlr3*, *Trpv1*, and *Myd88*) were obtained from Jackson Laboratories. All the knockout mice were viable and showed no developmental defects. Young mice (4–5 weeks) were used for electrophysiological studies in DRG neurons. Adult male mice (8–10 weeks) of knockout mice and corresponding wild-type control mice, as well as CD1 mice, were used for behavioral and pharmacological studies. All the animal procedures were approved by the Institutional Animal Care & Use Committee of Duke University.

## Whole-Cell and Inside-Out Single-Channel Recordings

Whole-cell patch-clamp recordings in DRG neurons (small sizes,  $<25 \mu\text{m}$ ) and HEK293 cells were performed at room temperature using an Axopatch-200B amplifier. To record inward currents, we conducted voltage clamp at holding membrane potential of  $-70 \text{ mV}$ . Inside-out patch-clamp recordings were also performed at room temperature.

## Pain Behavior Test

Intraplantar injection ( $10 \mu\text{l}$ ) was made by a 27G needle. miRNA-evoked spontaneous pain was assessed by measuring the time (seconds) mice spent on licking, lifting, or flinching the affected paw in 5 min. All the behaviors were tested blindly.

## Statistical analyses

All data were expressed as mean  $\pm$  SEM and analyzed using Student's *t* test (two groups) or one-way ANOVA followed by post hoc Bonferroni test. The criterion for statistical significance was  $p < 0.05$ .

## SUPPLEMENTAL INFORMATION

Supplemental Information includes Supplemental Experimental Procedures, two tables, and four figures and can be found with this article online at <http://dx.doi.org/10.1016/j.neuron.2014.02.011>.

## AUTHOR CONTRIBUTIONS

C.-K.P. performed electrophysiological and single-cell PCR studies; Z.-Z.X. performed behavioral studies; T.B. measured miRNA expression and release and performed in situ hybridization; Q.H. conducted binding and Co-IP experiments; G.C. performed TRPA1 staining in DRG neurons; X.-J.L. conducted transfection experiments; R.-R.J. formulated the hypotheses, supervised the project, and prepared the manuscript.

## Figure 4. Activity-Dependent Release of let-7b in DRG Cultures and Involvement of Endogenous let-7b in TRPA1 Function and Inflammatory Pain

(A) Inhibition of formalin (0.01%) induced inward currents by let-7b inhibitor (anti-mmu-let-7b-5p,  $1 \mu\text{M}$ ). Right: amplitude of formalin-induced currents after being normalized to control. \* $p < 0.05$ ,  $n = 12$ –15 neurons. (B) Blockade of let-7b- but not miR-599-induced currents in AITC-sensitive DRG neurons by let-7b inhibitor.  $n = 7$ –8 neurons. (C) let-7b expression levels in DRG, spinal cord, cortex, and skin tissues, assessed by quantitative RT-PCR and normalized to miRNA SNORD96A (a housekeeping miRNA). \* $p < 0.05$ , compared to spinal cord, cortex, and skin,  $n = 3$  mice. (D) let-7b release in DRG cultures at different neuronal densities before and after formalin treatment (0.01%, 30 min). let-7b levels in culture medium were assessed by quantitative RT-PCR and normalized to spike-in cel-miRNA-39. \* $p < 0.05$ , two-way ANOVA,  $n = 3$  cultures. (E) let-7b and let-7a release (fold of control) in DRG culture medium following 30 min treatment of formalin (0.01%), ionomycin (10 ng/ml), KCl (50 mM), capsaicin ( $1 \mu\text{M}$ ), AITC (300  $\mu\text{M}$ ), or chloroquine (1 mM). \* $p < 0.05$ , compared to control,  $n = 4$ –12 cultures. (F) let-7b-induced spontaneous pain at different doses. \* $p < 0.05$ , versus vehicle; # $p < 0.05$ , n.s., not significant. (G and H) Reduction of let-7b (30  $\mu\text{g}$ )-induced spontaneous pain in *Trpa1*<sup>-/-</sup>, *Tlr7*<sup>-/-</sup>, and *Myd88*<sup>-/-</sup> mice but not in *Trpv1*<sup>-/-</sup> mice. \* $p < 0.05$ , versus WT control; # $p < 0.05$ . (I) Dose-dependent inhibition of let-7b-evoked spontaneous pain by intraplantar HC030031 (1, 10  $\mu\text{g}$ ). \* $p < 0.05$ , versus let-7b vehicle (RNase free-water); # $p < 0.05$ , versus HC030031 vehicle (5% DMSO, green bar). (J) Low-dose let-7b (1  $\mu\text{g}$ ) induced mechanical allodynia in WT mice and *Trpa1*<sup>-/-</sup> mice. \* $p < 0.05$ ; # $p < 0.05$ . (K and L) High-dose let-7b (30  $\mu\text{g}$ ) induced mechanical allodynia in WT mice and *Tlr7*<sup>-/-</sup> (K) and *Trpa1*<sup>-/-</sup> (L) mice. \* $p < 0.05$ ; # $p < 0.05$ . (M) Inhibition of formalin (0.5%) induced pain in phase I (0–10 min) and phase II (10–45 min) by intraplantar let-7b inhibitor (3 nmol). \* $p < 0.05$ . (N) Formalin (0.5%) induced pain in phase I (0–10 min) and phase II (10–45 min) in WT and *Tlr7*<sup>-/-</sup> mice. \* $p < 0.05$ . The data are represented as mean  $\pm$  SEM;  $n = 5$ –11 mice for behavioral studies in (F)–(N).

## ACKNOWLEDGMENTS

We thank Dr. Ardem Patapoutian for providing TRPA1 antibody, Dr. Sun Wook Hwang for providing Trpa1, Trpv1, Trpv2, and Trpv4 constructors, and Dr. Jorg Grandl for critical reading of the manuscript. This study was supported by NIH R01 grants DE17794, DE22743, and NS67686 to R.-R.J. and NIH R21 grant NS82985 to Z.-Z.X. T.B. was supported by fellowships (PBLAP3-123417 and PA00P3-134165) from Switzerland.

Accepted: January 28, 2014

Published: April 2, 2014

## REFERENCES

- Akira, S., Uematsu, S., and Takeuchi, O. (2006). Pathogen recognition and innate immunity. *Cell* 124, 783–801.
- Bartel, D.P. (2004). MicroRNAs: genomics, biogenesis, mechanism, and function. *Cell* 116, 281–297.
- Basbaum, A.I., Bautista, D.M., Scherrer, G., and Julius, D. (2009). Cellular and molecular mechanisms of pain. *Cell* 139, 267–284.
- Bautista, D.M., Jordt, S.E., Nikai, T., Tsuruda, P.R., Read, A.J., Poblete, J., Yamoah, E.N., Basbaum, A.I., and Julius, D. (2006). TRPA1 mediates the inflammatory actions of environmental irritants and proalgesic agents. *Cell* 124, 1269–1282.
- Caterina, M.J., and Julius, D. (2001). The vanilloid receptor: a molecular gateway to the pain pathway. *Annu. Rev. Neurosci.* 24, 487–517.
- Eacker, S.M., Dawson, T.M., and Dawson, V.L. (2009). Understanding microRNAs in neurodegeneration. *Nat. Rev. Neurosci.* 10, 837–841.
- Fabbri, M., Paone, A., Calore, F., Galli, R., Gaudio, E., Santhanam, R., Lovat, F., Fadda, P., Mao, C., Nuovo, G.J., et al. (2012). MicroRNAs bind to Toll-like receptors to induce prometastatic inflammatory response. *Proc. Natl. Acad. Sci. USA* 109, E2110–E2116.
- Heil, F., Hemmi, H., Hochrein, H., Ampenberger, F., Kirschning, C., Akira, S., Lipford, G., Wagner, H., and Bauer, S. (2004). Species-specific recognition of single-stranded RNA via toll-like receptor 7 and 8. *Science* 303, 1526–1529.
- Hucho, T., and Levine, J.D. (2007). Signaling pathways in sensitization: toward a nociceptor cell biology. *Neuron* 55, 365–376.
- Jordt, S.E., Bautista, D.M., Chuang, H.H., McKemy, D.D., Zygmunt, P.M., Högestätt, E.D., Meng, I.D., and Julius, D. (2004). Mustard oils and cannabinoids excite sensory nerve fibres through the TRP channel ANKTM1. *Nature* 427, 260–265.
- Kang, K., Pulver, S.R., Panzano, V.C., Chang, E.C., Griffith, L.C., Theobald, D.L., and Garrity, P.A. (2010). Analysis of *Drosophila* TRPA1 reveals an ancient origin for human chemical nociception. *Nature* 464, 597–600.
- Lehmann, S.M., Krüger, C., Park, B., Derkow, K., Rosenberger, K., Baumgart, J., Trimbuch, T., Eom, G., Hinz, M., Kaul, D., et al. (2012). An unconventional role for miRNA: let-7 activates Toll-like receptor 7 and causes neurodegeneration. *Nat. Neurosci.* 15, 827–835.
- Liu, T., and Ji, R.R. (2013). New insights into the mechanisms of itch: are pain and itch controlled by distinct mechanisms? *Pflugers Arch.* 465, 1671–1685.
- Liu, T., Xu, Z.Z., Park, C.K., Berta, T., and Ji, R.R. (2010). Toll-like receptor 7 mediates pruritus. *Nat. Neurosci.* 13, 1460–1462.
- Liu, T., Berta, T., Xu, Z.Z., Park, C.K., Zhang, L., Lü, N., Liu, Q., Liu, Y., Gao, Y.J., Liu, Y.C., et al. (2012a). TLR3 deficiency impairs spinal cord synaptic transmission, central sensitization, and pruritus in mice. *J. Clin. Invest.* 122, 2195–2207.
- Liu, T., Gao, Y.J., and Ji, R.R. (2012b). Emerging role of Toll-like receptors in the control of pain and itch. *Neurosci. Bull.* 28, 131–144.
- Macpherson, L.J., Dubin, A.E., Evans, M.J., Marr, F., Schultz, P.G., Cravatt, B.F., and Patapoutian, A. (2007). Noxious compounds activate TRPA1 ion channels through covalent modification of cysteines. *Nature* 445, 541–545.
- McNamara, C.R., Mandel-Brehm, J., Bautista, D.M., Siemens, J., Deranian, K.L., Zhao, M., Hayward, N.J., Chong, J.A., Julius, D., Moran, M.M., and Fanger, C.M. (2007). TRPA1 mediates formalin-induced pain. *Proc. Natl. Acad. Sci. USA* 104, 13525–13530.
- Orlova, I.A., Alexander, G.M., Qureshi, R.A., Sacan, A., Graziano, A., Barrett, J.E., Schwartzman, R.J., and Ajit, S.K. (2011). MicroRNA modulation in complex regional pain syndrome. *J. Transl. Med.* 9, 195.
- Pasquinelli, A.E., Reinhart, B.J., Slack, F., Martindale, M.Q., Kuroda, M.I., Maller, B., Hayward, D.C., Ball, E.E., Degnan, B., Müller, P., et al. (2000). Conservation of the sequence and temporal expression of let-7 heterochronic regulatory RNA. *Nature* 408, 86–89.
- Patapoutian, A., Tate, S., and Woolf, C.J. (2009). Transient receptor potential channels: targeting pain at the source. *Nat. Rev. Drug Discov.* 8, 55–68.
- Qin, N., Neeper, M.P., Liu, Y., Hutchinson, T.L., Lubin, M.L., and Flores, C.M. (2008). TRPV2 is activated by cannabidiol and mediates CGRP release in cultured rat dorsal root ganglion neurons. *J. Neurosci.* 28, 6231–6238.
- Reinhart, B.J., Slack, F.J., Basson, M., Pasquinelli, A.E., Bettinger, J.C., Rougvie, A.E., Horvitz, H.R., and Ruvkun, G. (2000). The 21-nucleotide let-7 RNA regulates developmental timing in *Caenorhabditis elegans*. *Nature* 403, 901–906.
- Schmidt, M., Dubin, A.E., Petrus, M.J., Earley, T.J., and Patapoutian, A. (2009). Nociceptive signals induce trafficking of TRPA1 to the plasma membrane. *Neuron* 64, 498–509.
- Story, G.M., Peier, A.M., Reeve, A.J., Eid, S.R., Mosbacher, J., Hricik, T.R., Earley, T.J., Hergarden, A.C., Andersson, D.A., Hwang, S.W., et al. (2003). ANKTM1, a TRP-like channel expressed in nociceptive neurons, is activated by cold temperatures. *Cell* 112, 819–829.
- Takeuchi, O., and Akira, S. (2010). Pattern recognition receptors and inflammation. *Cell* 140, 805–820.
- von Schack, D., Agostino, M.J., Murray, B.S., Li, Y., Reddy, P.S., Chen, J., Choe, S.E., Strassle, B.W., Li, C., Bates, B., et al. (2011). Dynamic changes in the microRNA expression profile reveal multiple regulatory mechanisms in the spinal nerve ligation model of neuropathic pain. *PLoS ONE* 6, e17670.
- Woolf, C.J., and Ma, Q. (2007). Nociceptors—noxious stimulus detectors. *Neuron* 55, 353–364.
- Zhao, J., Lee, M.C., Momin, A., Cendan, C.M., Shepherd, S.T., Baker, M.D., Asante, C., Bee, L., Bethry, A., Perkins, J.R., et al. (2010). Small RNAs control sodium channel expression, nociceptor excitability, and pain thresholds. *J. Neurosci.* 30, 10860–10871.

Neuron, Volume 82

Supplemental Information

## **Extracellular MicroRNAs Activate Nociceptor**

### **Neurons to Elicit Pain via TLR7 and TRPA1**

Chul-Kyu Park, Zhen-Zhong Xu, Temugin Berta, Qingjian Han, Gang Chen, Xing-Jun Liu,  
and Ru-Rong Ji

## **I. Supplemental Experimental Procedures**

### **Reagents**

We purchased miRNAs from Integrated DNA Technologies. The sequences of miRNAs and control mutant oligoribonucleotide (Mut. oligo) (Lehmann et al., 2012) are shown in Figure 1. The Mut. Oligo has reduced GU content but no changes in the 5' let-7 seed sequence that is important for post-transcriptional silencing. Fluorescence-conjugated siRNA (Cy3-let-7b) and HC030031 were from Sigma. The inhibitor of let-7b (Lehmann et al., 2012) and kit for measuring miRNAs were from Qiagen.

### **Animals**

Knockout mice lacking *Tlr7*, *Tlr3*, *Trpa1*, *Trpv1*, and *Myd88* and corresponding WT control mice (B6129PF2/J background for *Trpa1*; C57BL/6 background for *Tlr7*, *Tlr3*, *Trpv1*, and *Myd88*) were purchased from Jackson Laboratories and maintained at Duke animal facility. All the knockout mice were viable and showed no developmental defects. Young mice (4-5 weeks) were used for electrophysiological studies in DRG neurons. Adult male mice (8-10 weeks) of knockout mice and corresponding wild-type control mice, as well as CD1 mice were used for behavioral and pharmacological studies. All the animal procedures were approved by the Institutional Animal Care & Use Committee of Duke University.

### **HEK293 cells and transfection**

HEK293 and HEK293XL-mTLR7 cell lines were purchased from InvivoGen. Cells were cultured in high glucose (4.5 g/L) Dulbecco's Modified Eagle's Medium containing 10% (v/v) fetal bovine serum (Gibco). HEK293XL-mTLR7 cells were maintained and subcultured in a growth medium supplemented with 10 µg/ml Blastidin. Transfection (2 µg cDNA) was performed with Lipofectamine<sup>TM</sup> 2000 Reagent (Invitrogen) at 80% confluency and the transfected cells were cultured in the same growth medium for 48 h before electrophysiological and biochemical studies. pcDNA3.1-mTRPA1-myc-His plasmid was kindly provided by Ardem Patapoutian from The Scripps Research Institute and the cDNAs of *Trpa1*, *Trpv1*, *Trpv2*, and *Trpv4* were kindly provided Dr. Sun Work Hwang from Korea University.

### **Primary cultures of DRG neurons**

DRGs were removed aseptically from mice (4-6 weeks) and incubated with collagenase (1.25mg/ml, Roche)/dispase-II (2.4 units/ml, Roche) at 37°C for 90 min, then digested with 0.25% trypsin for 8 min at 37°C, followed by 0.25% trypsin inhibitor. Cells were mechanically dissociated with a flame polished Pasteur pipette in the presence of 0.05% DNase I (Sigma). DRG cells were plated on glass cover slips and grown in a neurobasal defined medium (with 2% B27 supplement, Invitrogen) with 5  $\mu$ M AraC and 5% carbon dioxide at 36.5°C. DRG neurons were grown for 24 hours before use.

### **Whole-cell and inside-out single channel recordings in DRG neurons and HEK293 cells**

Whole-cell and inside-out patch clamp recordings were performed at room temperature using an Axopatch-200B amplifier (Axon Instruments). The patch pipettes were pulled from borosilicate capillaries (Chase Scientific Glass Inc.). Pipette resistance was 4-6 M $\Omega$  for whole-cell recording or 7-9 M $\Omega$  for inside-out recording, and the internal solution contains (in mM): 126 K-gluconate, 10 NaCl, 1 MgCl<sub>2</sub>, 10 EGTA, 2 NaATP, and 0.1 MgGTP, adjusted to pH 7.3 with KOH and osmolarity 295-300 mOsm. Whole cell recordings were performed in an extracellular solution (in mM): 140 NaCl, 5 EGTA, 5 KCl, 2 CaCl<sub>2</sub>, 1 MgCl<sub>2</sub>, 10 HEPES, 10 glucose, adjusted to pH 7.4 with NaOH and osmolarity 300-310 mOsm.

Inside-out patch recordings were performed at room temperature in a bath solution (intracellular side) (in mM): 140 NaCl, 10 EGTA, 5 KCl, 2 CaCl<sub>2</sub>, 1 MgCl<sub>2</sub>, 10 HEPES, 10 glucose, adjusted to pH 7.4 with NaOH and osmolarity 300-310 mOsm. Currents were low-pass filtered at 1 kHz in whole-cell recordings and at 3 kHz in single-channel recordings. Currents were digitized at a sampling rate of 3 kHz in whole-cell recordings and 10 kHz in single channel recordings with Digidata-1440A (Axon Instruments). The pClamp10 (Axon Instruments) software was used during experiments and data analysis. Opening and closing transitions of single channels were detected by using 50% of the threshold criterion. All events were carefully checked before the analysis. Amplitude histograms were obtained using Clampfit software. Single-channel amplitude was calculated from the difference between gauss fitted “closed” and “open” peaks. When superimposed openings were observed, the number of channels in the patch was estimated from the maximal number of superimposed openings. The single-channel open

probability ( $P_o$ ) for the inside-out patches was determined using the following equation:  $P_o = T'/T$ , where  $T'$  is the total open time for a patch over time  $T$ .

### **Immunocytochemistry**

To determine the surface expression of TRPA1, cultured DRG neurons from WT and *Tlr7* knockout mice were stimulated with mustard oil (AITC; 150  $\mu$ M, 10 min) and then were incubated with anti-TRPA1 antibody (AbE3, 1:50; kindly provided by Dr. Patapoutian A) (Schmidt et al., 2009) for 10 min at 37°C. Cells were then incubated with Cy3-conjugated secondary antibodies (1:400; Jackson ImmunoResearch) for 10 min at room temperature. Finally cells were fixed with 2% paraformaldehyde and examined with a Nikon fluorescence microscope. The percentage of TRPA1-positive neuron was calculated from 200 randomly selected neurons and three independent preparations were included.

293XL-hTLR7 cells were cultured on coverslips, and transfected with pcDNA3.1-mTRPA1-myc-His plasmid, 48 hours later, transfected cells were stimulated 50  $\mu$ g/ml cy3 labeled let-7b or vehicle for 5 min fixed with 4% paraformaldehyde for 15 min and incubated overnight with a rabbit antibody against TLR7 (1:1000; IMGENEX) mixed with a mouse antibody against myc (1:500; Millipore, Billerica, MA). Then, the cells on coverslips were incubated with secondary antibodies conjugated to FITC and Cy5 (1:100; Jackson ImmunoResearch, West Grove, PA) and examined under a Zeiss LSM 510 inverted confocal microscope (North Chesterfield, VA).

### **Immunoprecipitation and immunoblotting**

Transfected 293XL-hTLR7 cells were stimulated 50  $\mu$ g/ml let-7b or vehicle for 5 min and lysed in ice-cold immunoprecipitation buffer (10 mM TrisHCl, pH 7.4, 150 mM NaCl, 1 mM EDTA, 1% Triton X-100 and 10% glycerol). The lysate was immunoprecipitated with 0.5 mg mouse antibody against myc (Millipore, Billerica, MA) and then incubated with protein G-Sepharose beads (Roche, Mannheim, Germany). For immunoblotting, the lysates or beads were incubated in SDS-PAGE loading buffer. The samples were separated on an SDS-PAGE gel, transferred, and probed with antibodies against TLR7 (1:2000; IMGENEX, San Diego, CA), myc (1:1000; Millipore). The immunoreactive bands were then detected with horseradish peroxidase-conjugated secondary antibodies, visualized with enhanced chemiluminescence (Thermo

scientific, Pittsburgh, PA) and quantified with Image-Pro Plus software (Media Cybernetics Inc., Bethesda, MD). Each experiment was repeated at least three times.

### **Fluorescent In situ Hybridization (FISH) and Immunohistochemistry (IHC)**

DRGs were dissected from 4% paraformaldehyde transcardially perfused mice. FISH were carried out according to the manufacturer's guide. Briefly, sections of 10- $\mu$ m thickness were permeabilized with 70% ethanol and incubated with multiple oligonucleotide probes targeting TRPA1 (Stellaris FISH probes labeled with Quasar® 570 Dye, BioResearch Technologies) overnight at 37°C. Sections were then washed and incubated overnight with rabbit TLR7 primary antibody (Imgenex) at 4°C following a standard IHC. TLR7 signal was detected by incubation with FITC-conjugated antibody against rabbit (Jackson Laboratories). Images of were acquired with Nikon fluorescence microscopes (Nikon) and FISH and IHC signals superposed by Photoshop (Adobe).

### **Single-cell RT-PCR**

As described in (Liu et al., 2012), a single cell was aspirated into a patch pipette, gently put into a reaction tube containing reverse transcription reagents, and incubated for 1 hr at 50°C (superscript III, Invitrogen). The cDNA product was then used in separate PCR. The sequences of all the primers used for single-cell PCR are described in Table-S2. The 1<sup>st</sup> and 2<sup>nd</sup> round PCR was performed using “outer” primers and “inner” primers, respectively. A negative control was obtained from pipettes that did not harvest any cell contents. The PCR products were displayed on ethidium bromide-stained 1.5 % agarose gels.

### **miRNA quantification by quantitative real-time RT-PCR (qPCR)**

Total RNA was isolated from cortex, spinal cord, DRG and skin tissues using Qiazol Lysis Reagent (Qiagen) together with miRNeasy Kit (Qiagen). All RNA samples were immediately used or kept at -80°C until further processing. To convert mature miRNA into cDNA, 6  $\mu$ l of total RNA solution were reverse transcribed using the miScript II RT Kit (including polyadenylation of miRNAs and reverse transcription using an oligo-dT that binds to an universal RT-sequence, Qiagen). Specific miRNA levels were quantified by qPCR using miScript SYBR Green Kit [Qiagen, including miScript miRNA assay for mmu-let-7b (assay ID

MS00001225) and mmu-let-7a (assay ID MS000032179), together with the universal RT primer], according to the manufacturer's protocol (CFX96 Real-Time system, Bio-Rad). Relative quantities of miRNAs were calculated using the Ct method after normalization to control miRNAs. mmu-SNORD96A (assay ID MS00033733) was used as control for intracellular miRNA, because of its ubiquitous and stable expression in various tissues and cell types (Qiagen). *Caenorhabditis elegans* miRNA-39 (cel-miRNA-39) was included as spiked-in control for extracellular miRNA.

To measure miRNA release, DRG neurons were cultured in 12-well plates at densities of 1500-5000 neurons/well for testing the density-dependent effects of let-7b release and also at the density of 5000 neurons/well for testing the activity-dependent release of let-7a and let-7b. Before the stimulation, DRG cultures were washed three times in Krebs solution. Cells were then incubated with 200  $\mu$ l of Krebs solution containing formalin (0.01%), ionomycin (10 ng/ml), KCl (50 mM), capsaicin (1  $\mu$ M), AITC (300 mM), and chloroquine (1 mM) for 30 min at 37°C. Supernatants were harvested and cleared of debris by centrifugation (12000 g for 20 min at 4°C). Isolation of extracellular miRNAs from supernatants was performed using Qiazol Lysis Reagent (Qiagen) together with miRNeasy Serum/Plasma Kit (Qiagen). The concentration of let-7b (pg/ml) was calculated based on a standard curve obtained from synthetic let-7b (Integrated DNA Technologies) and the Ct values were plotted as described previously (Kroh, et al., 2010).

## References

Kroh EM, Parkin RK, Mitchell PS, Tewari M (2010) Analysis of circulating microRNA biomarkers in plasma and serum using quantitative reverse transcription-PCR (qRT-PCR). *Methods* 50:298-301.

Lehmann,S.M., Kruger,C., Park,B., Derkow,K., Rosenberger,K., Baumgart,J., Trimbuch,T., Eom,G., Hinz,M., Kaul,D., Habel,P., Kalin,R., Franzoni,E., Rybak,A., Nguyen,D., Veh,R., Ninnemann,O., Peters,O., Nitsch,R., Heppner,F.L., Golenbock,D., Schott,E., Ploegh,H.L., Wulczyn,F.G., and Lehnardt,S. (2012). An unconventional role for miRNA: let-7 activates Toll-like receptor 7 and causes neurodegeneration. *Nat. Neurosci* 15, 827-835.

Liu,T., Berta,T., Xu,Z.Z., Park,C.K., Zhang,L., Lu,N., Liu,Q., Liu,Y., Gao,Y.J., Liu,Y.C., Ma,Q., Dong,X., and Ji,R.R. (2012). TLR3 deficiency impairs spinal cord synaptic transmission, central sensitization, and pruritus in mice. *J Clin. Invest* 122, 2195-2207.

## II. Supplemental Tables

**Supplemental Table-1.** The GUUGUGU motif contained in miRNAs of Homo sapiens and Mus musculus (related to Figure 1).

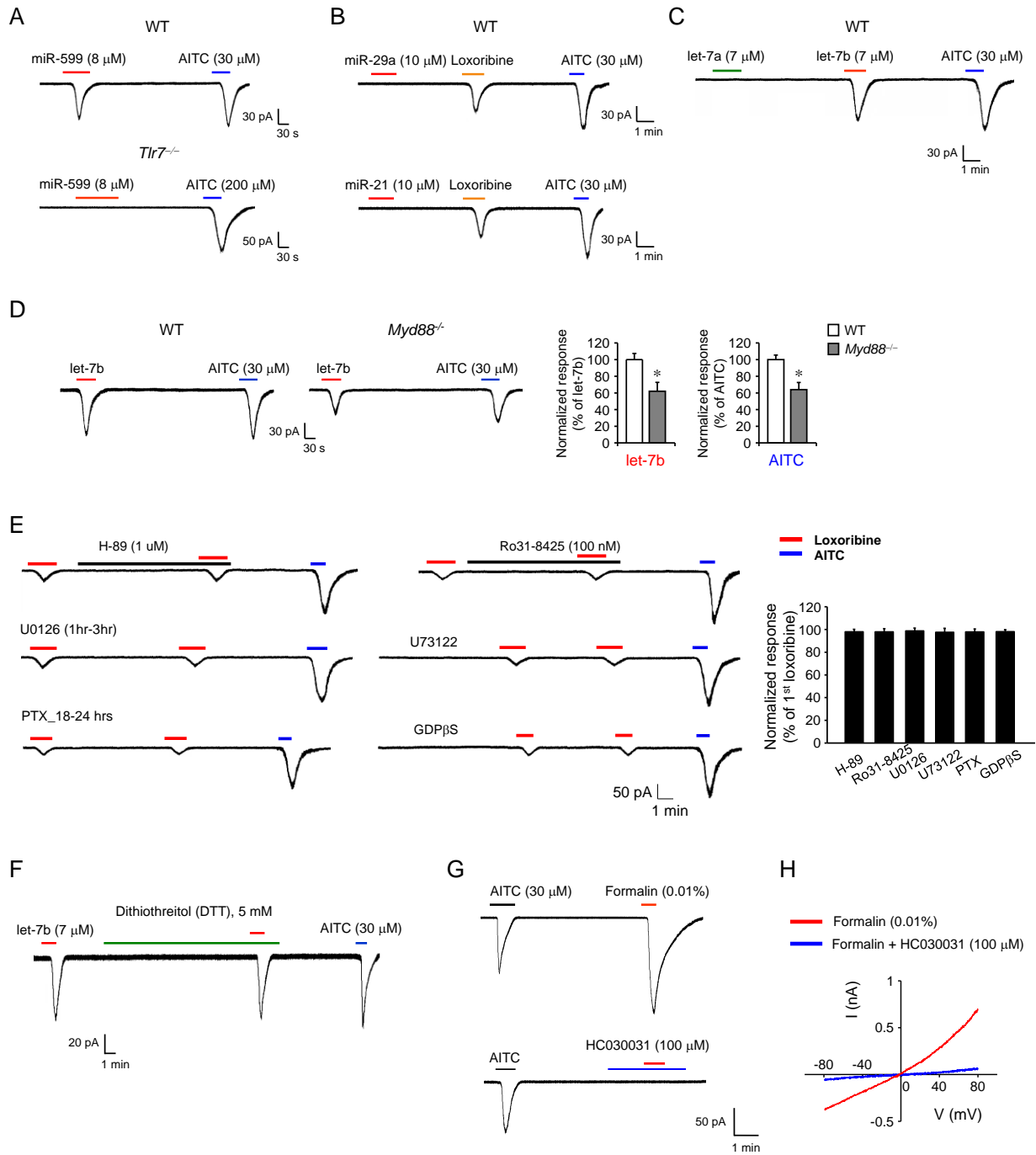
<b>miRNA</b>	<b>Sequence</b>
<u>Homo sapiens</u>	
hsa-let-7b-5p	UGAGGUAGUAG <b>GUUGUGU</b> GGUU
hsa-miR-599	<b>GUUGUGU</b> CAGUUUAUCAAC
<u>Mus musculus</u>	
mmu-let-7b-5p	UGAGGUAGUAG <b>GUUGUGU</b> GGUU
mmu-let-7k	UGAGGUAGGAG <b>GUUGUGU</b> G
mmu-miR-669a-5p	<b>AGUUGUGU</b> GUGCAUGUUCAUGUCU
mmu-miR-669c-5p	AU <b>AGUUGUGU</b> GUGGAUGUGUGU
mmu-miR-669f-5p	<b>AGUUGUGU</b> GUGCAUGUGCAUGUGU
mmu-miR-669k-5p	UGUGCAUGUGUGUAUA <b>GUUGUGU</b> GC
mmu-miR-669l-5p	<b>AGUUGUGU</b> GUGCAUGUAUAUGU
mmu-miR-669o-5p	UA <b>GUUGUGU</b> GUGCAUGUUUAUGU
mmu-miR-669p-5p	<b>AGUUGUGU</b> GUGCAUGUUCAUGUCU

**Supplemental Table-2.** Sequences of outer and inner primers for single-cell PCR (related to Figure 1).

Target gene (Product length) <sup>a</sup>	Outer primers	Inner primers	Genbank No.
TRPV1 (273 bp, 203 bp)	TGATCATCTCACCACGGCTG CCTTGCATGGCTGAAGTACA	AAGGCTTGCCCCCTATAA CACCAGCATGAACAGTGACTGT	NM_001001445.1
TRPA1 (371 bp, 303 bp)	GGCTTTTGGCCTCAGCTTTTAT ACACGATGGTGGACCTCTGATC	ATGCCTTCAGCACCCATT TGCCTAAGTACCAGAGTGGCAG	NM_177781.4
GAPDH (367 bp, 313 bp)	AGCCTCGTCCCCTAGACAAAA TTTTGGCTCCACCCCTTCA	TGAAGGTCGGTGTGAACGAATT GCTTTCTCCATGGTGGTGAAGA	XM_001473623.1
TLR7 (421 bp, 359 bp)	CAGTGA ACTCTGGCCGTTGAGA TGGCGGCATACCCTCAAAA	TTCTCCAACAACCGGCTTGAT TCAGGAGGCAAGGAATTCAGG	NM_133211.3

(n, n) indicates product size obtained from outer and inner primers, respectively.

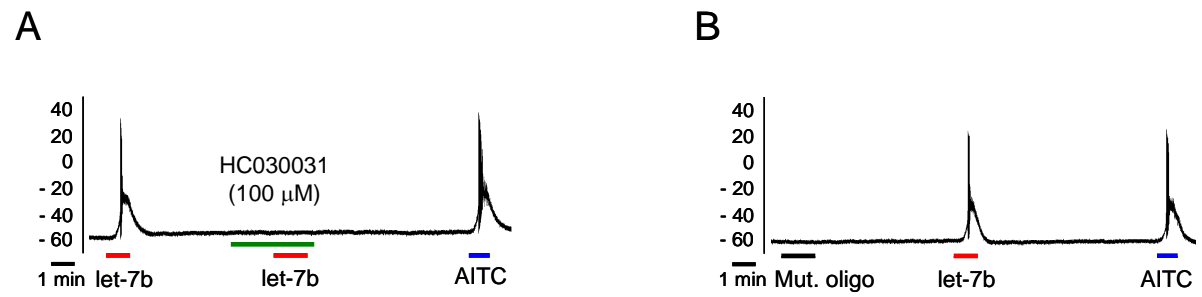
### III. Supplemental Figures



### Supplemental Figure 1. Inward currents in DRG neurons (related to Figure 1)

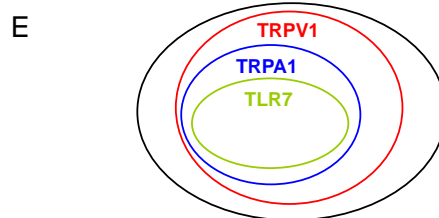
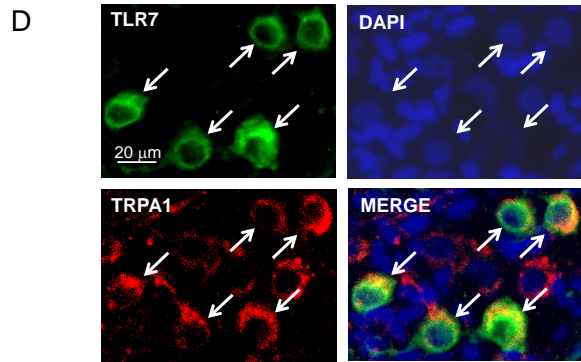
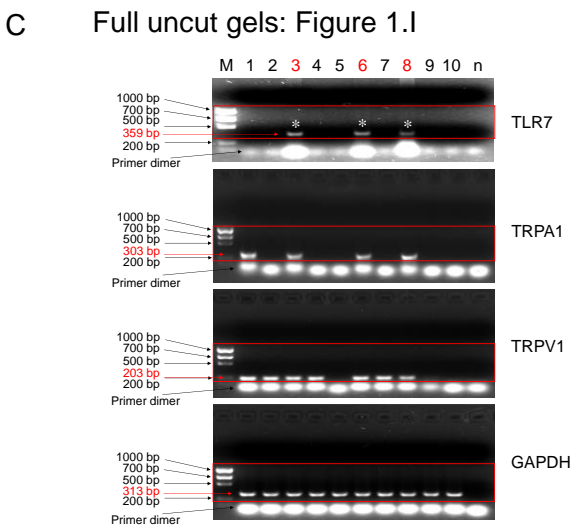
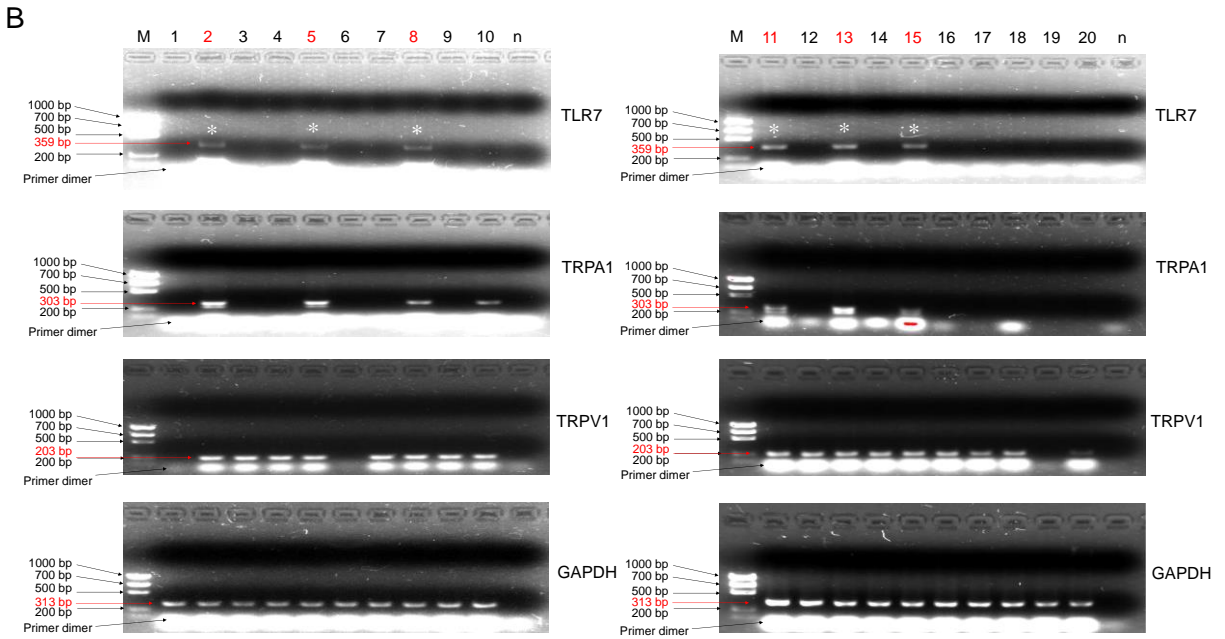
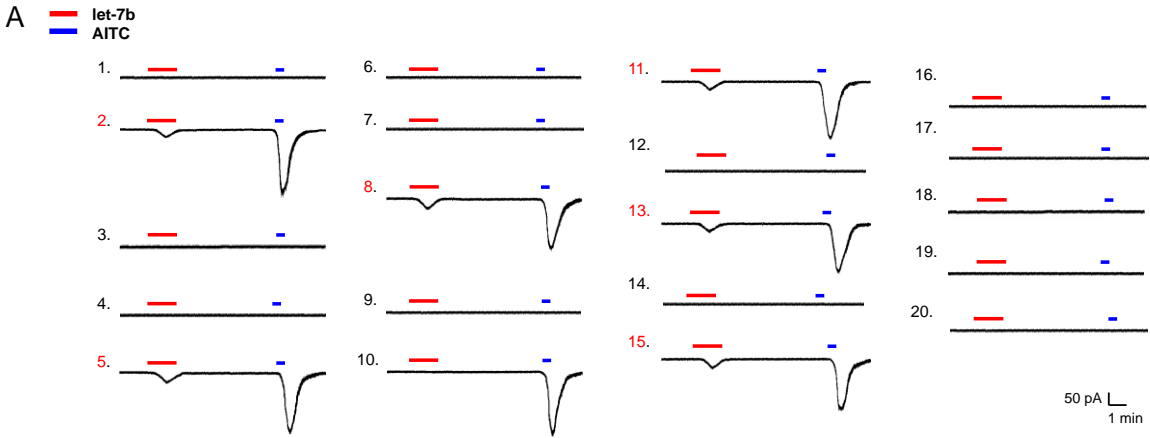
(A) miR-599 but not miR-29a and miR-21 induces inward currents in small-sized DRG neurons via TLR7. miR-599 (8  $\mu$ M) induces AITC-sensitive inward currents in DRG neurons (7 out of 24) of WT but not *Tlr7*<sup>-/-</sup> mice (n = 0/25). (B) miR-29a (10  $\mu$ M) and miR-21 (10  $\mu$ M) do not elicit inward currents in loxoribine- and AITC-sensitive DRG neurons (n = 0/25). (C) let-7a (7  $\mu$ M) fails to induce any inward current in let-7b- and AITC-sensitive DRG neurons (n = 0/10). (D) Myd88 is partially required for let-7b-induced inward currents in small-sized DRG neurons. Left, traces of let-7b-induced inward currents. Right, the amplitudes of let-7b (7  $\mu$ M) and AITC (30  $\mu$ M)-induced inward currents are slightly reduced in *Myd88*<sup>-/-</sup> mice ( $\approx$ 30% reduction,  $P < 0.05$ , *t*-test, compared with WT mice; n = 6 neurons). (E) Intracellular signaling pathways are not required for the functional coupling of TLR7 and TRPA1 in DRG neurons. Loxoribine (200  $\mu$ M)-induced inward currents are not suppressed by inhibitors of PKA (H-89, 1  $\mu$ M, n = 15), PKC (Ro31-8425, 100 nM, n = 12), ERK (U0126, 10  $\mu$ M, n = 9), PLC (U73122, 10  $\mu$ M, n = 8), and G-proteins (pertussis toxin, 0.5  $\mu$ g/ml, n = 8; GDP  $\beta$ S, 2.5 mM, n = 8). Right, peak amplitude of loxoribine-induced currents in DRG neurons following the treatment of the above-mentioned inhibitors. The data are normalized to the peak amplitude of the first loxoribine response ( $P > 0.05$ ; paired *t*-test versus first loxoribine response). DRG neurons were treated with the inhibitors for 5-6 min before the 2<sup>nd</sup> loxoribine stimulation. (F) Treatment of DRG neurons with dithiothreitol (5 mM, 10 min), a cell-permeable reducing agent, does not alter let-7b (7  $\mu$ M)-induced inward currents. n = 6 neurons. (G) Low concentration of formalin (0.01%) induces TRPA1-mediated inward currents in DRG neurons (n = 8). The formalin-induced inward currents are completely blocked by the TRPA1 antagonist HC030031 (100  $\mu$ M, n = 7). (H) Formalin (0.01%) induced I/V curves with the reversal potential of 0 mV (n = 5). Formalin-induced current is suppressed by HC030031 (100  $\mu$ M, n = 5). All the data are mean  $\pm$  SEM.

**Fig. S2**



**Supplementary Figure 2. Action potentials in DRG neurons (related to Figure 1).**

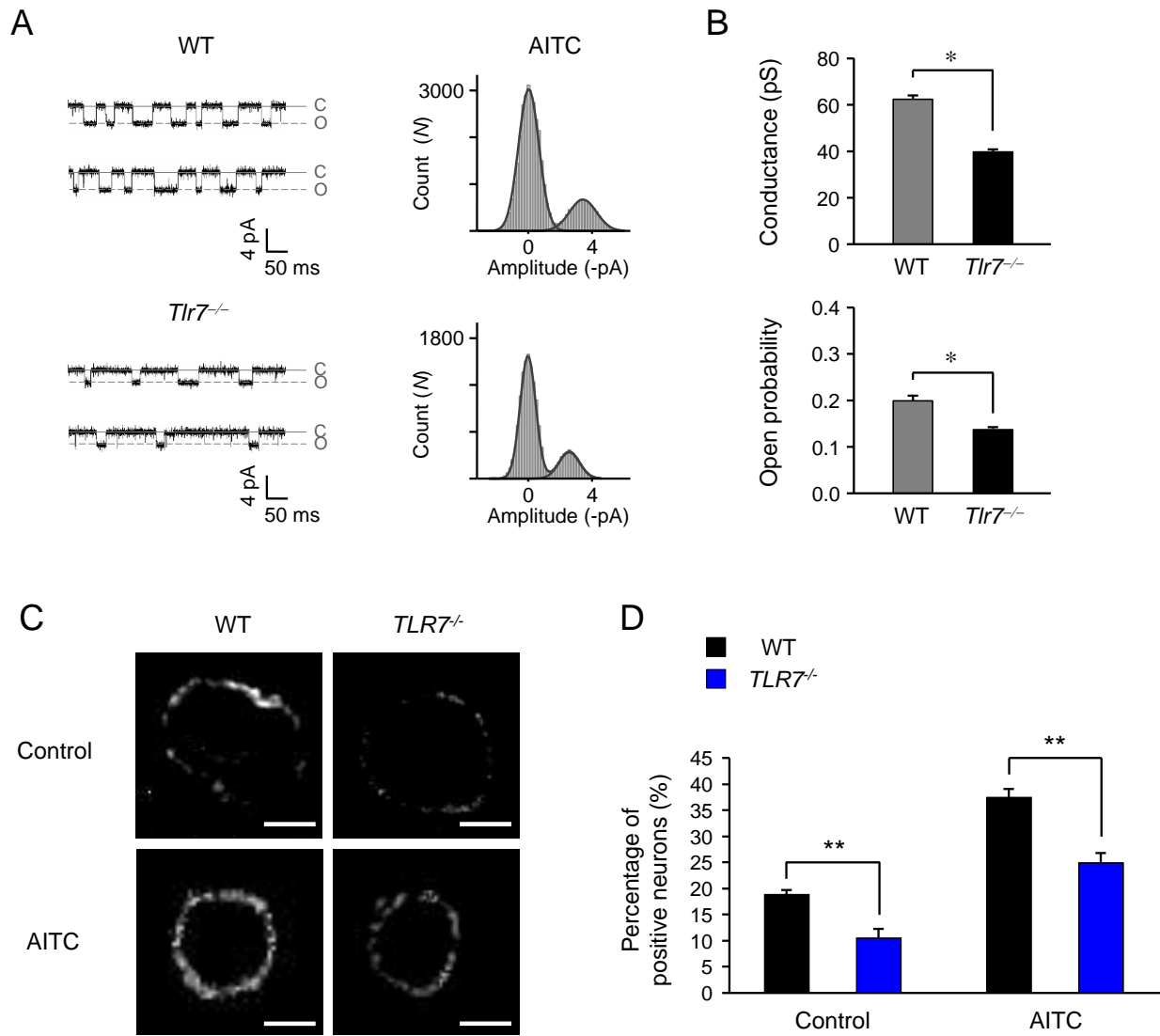
(A) let-7b-induced action potentials are blocked by HC030031 (100  $\mu$ M). (B) Action potentials induced by let-7b and AITC but not by Mut. oligo in DRG neurons. n = 5-10 neurons.



**Supplemental Figure 3. let-7b induces inward currents in small-diameter DRG neurons that co-express TLR7 and TRPA1 (related to Figure 1).**

**(A and B)** Inward currents (A) and single-cell RT-PCR (B) in 20 small-sized DRG neurons. Note that let-7b induces inward currents exclusively in TLR7-expressing neurons. Six neurons (#2, 5, 8, 11, 13, and 15, highlighted in red) respond to let-7b (7  $\mu$ M) by displaying inward currents, and these neurons also express *Tlr7*, *Trpa1*, and *Trpv1* mRNAs. M, molecular weights; n, negative control. Asterisks indicate TLR7-positive neurons. **(C)** Full uncut gels of Figure 1I. The molecular weights for specific bands are highlighted in red. **(D)** Double staining of TLR7 immunofluorescence (green) and TRPA1 in situ hybridization (red) in DRG sections shows colocalization of TLR7 and TRPA1. Arrows indicate double-labeled neurons with TLR7 and TRPA1. The nuclei were stained with DAPI. **(E)** Venn diagram shows the relationship of TLR7+, TRPA1+, and TRPV1+ populations in DRG. Note that all TLR7+ cells express TRPA1 and TRPV1 and all TRPA1+ cells express TRPV1.

**Fig. S4**



**Supplementary Figure 4. TRPA1 function and expression is impaired in DRG neurons of *Tlr7*<sup>-/-</sup> mice (related to Figure 2).**

**(A and B)** Inside-out patch recordings (-60 mV) in membrane excised from small-sized DRG neurons showing reduced TRPA1 single channel activity in *Tlr7*<sup>-/-</sup> mice. **(A)** Left, representative AITC (200  $\mu$ M)-activated single channel activities from wild-type and *Tlr7*<sup>-/-</sup> mice. Right, all-point histograms of single-channel opening events (5 min recordings) at -60 mV. The averages of single channel currents are  $-3.75 \pm 0.1$  pA and  $-2.4 \pm 0.07$  pA in wild-type and *Tlr7*<sup>-/-</sup> mice, respectively. **c:**

closed state; o: open state. (B) AITC-induced single channel conductance and open probability are reduced in *Tlr7*<sup>-/-</sup> mice. \**P* < 0.05, *t*-test. n = 7-8 neurons. (C and D) TRPA1 surface expression in DRG neurons, either before or after AITC-stimulation, is reduced in *Tlr7*<sup>-/-</sup> mice. (C) Immunocytochemistry showing TRPA1 expression in DRG neurons in WT and *Tlr7*<sup>-/-</sup> mice, before or after AITC stimulation. DRG neurons were stimulated with AITC (150 μM) for 10 min, and fresh (non-fixed) DRG neurons were incubated with TRPA1 antibody for 10 min, followed by Cy3-conjugated 2<sup>nd</sup> antibody. AITC increases TRPA1 surface expression, and both basal and AITC-induced TRPA1 surface expression are reduced in the KO mice (scale bar = 10 μm). (D) Percentage of TRPA1-positive DRG neurons in WT and *Tlr7*<sup>-/-</sup> mice, before or after AITC stimulation. \**P* < 0.05, *t*-test. n=4 cultures from separate experiments. All the data are mean ± SEM.